Title

Serum- and Glucocorticoid-Inducible Kinase 1 Promotes Alternative Macrophage Polarization and Restrains Inflammation through FoxO1 and STAT3 Signaling.

Journal

The Journal of Immunology, 207(1)

Authors

Ren, Junling

Han, Xiao

Lohner, Hannah

et al.

Publication Date

2021-07-01

DOI

10.4049/jimmunol.2001455

Peer reviewed

HHS Public Access

Author manuscript

J Immunol. Author manuscript; available in PMC 2022 July 01.

Published in final edited form as:

J Immunol. 2021 July 01; 207(1): 268–280. doi:10.4049/jimmunol.2001455.

Serum- and glucocorticoid-inducible kinase 1 promotes alternative macrophage polarization and restrains inflammation through FoxO1 and STAT3 signaling

Junling Ren[1], **Xiao Han**[1], **Hannah Lohner**[1], **Ruqiang Liang**[2], **Shuang Liang**[3], **Huizhi Wang**[1,*]

[1]VCU Philips Institute for Oral Health Research, Department of Oral and Craniofacial Molecular Biology, Virginia Commonwealth University, Richmond, VA, 23298, USA

[2]Department of Biochemistry and Molecular Medicine, University of California, Davis, Davis, CA, USA.

[3]Department of Basic Science and Craniofacial Biology, New York University College of Dentistry, New York, NY, 10010, USA.

Abstract

Expression and activity of serum- and glucocorticoid-inducible kinase 1 (SGK1) are associated with many metabolic and inflammatory diseases. Here, we report that SGK1 promotes alternative macrophage polarization and restrains inflammation in the infectious milieu of the gingiva. Inhibition of SGK1 expression or activity produces changes characteristic of M1 macrophages, by directly activating transcription of genes encoding iNOS, IL-12P40, TNFα, IL-6 and repressing IL-10 at message and protein levels. Moreover, SGK1 inhibition robustly reduces expression of M2 macrophage molecular markers including arginase-1, Ym-1, Fizz1, and Mgl1. These results were confirmed by multiple gain- and loss-of-function approaches including siRNA, a plasmid encoding SGK1, and *LysM*-Cre-mediated *sgk1* gene knockout. Further mechanistic analysis showed that SGK1 deficiency decreases STAT3 but increases FoxO1 expression in macrophages under M2 or M1 macrophage-priming conditions, respectively. Combined with decreased FoxO1 phosphorylation and subsequent suppressed cytoplasmic translocation observed, SGK1 deficiency robustly enhances FoxO1 activity and drives macrophage to preferential M1 phenotypes. Furthermore, FoxO1 inhibition abrogates M1 phenotypes and STAT3 overexpression results in a significant increase of M2 phenotypes, indicating that both FoxO1 and STAT3 are involved in SGK1-mediated macrophage polarization. Additionally, SGK1 differentially regulates expression of M1 and M2 molecular markers, including CD68 and F4/F80, and CD163 and CD206, respectively, and protects against *P. gingivalis*-induced alveolar bone loss in a mouse model. Taken together, we have demonstrated that SGK1 is critical for macrophage polarization

[*]**Correspondence:** Huizhi Wang, Ph.D.; M.D.; Associate Professor, VCU Philips Institute for Oral Health Research, Oral and Craniofacial Molecular Biology, School of Dentistry, Virginia Commonwealth University, Perkinson Bldg, Room 4152, 521 N. 11th St. Richmond, Virginia 23298-0566, wangh3@vcu.edu, Lab: (804) 628-6298, Office: (804) 628-6386, Fax: (804) 828-0150.

Authors' Contribution

J. Ren, X. Han, H. Lohner, and S. Liang performed research; J. Ren, S. Liang, and R. Liang analyzed the data; H. Wang designed the research, analyzed the data and wrote the paper. All authors read and approved the final manuscript.

Disclosures

The authors have no financial conflicts of interest.

and periodontal bone loss, and for the first time, we elucidated a bifurcated signaling circuit by which SGK1 promotes alternative, while suppressing inflammatory, macrophage polarization.

Keywords

SGK1; Macrophage polarization; *P. gingivalis* ; FoxO1; STAT3

Introduction

As a heterogeneous population of immune cells, macrophages are essential for the initiation, maintenance, and resolution of pathogen- or tissue damage- induced inflammation. Macrophages can be activated through diverse mechanisms and thus possess considerable plasticity (1, 2). In response to toll-like receptor (TLR)2/TLR4 and interferons (IFNs) engagement, macrophages undergo a classical activation and are polarized toward classic (M1) macrophages. On the other hand, alternative activation of macrophages, also called M2 macrophage polarization, can be induced by interleukin (IL)-4/IL-13 stimulation. Different populations of macrophages have distinct functions that are phenotypically characterized by the production of proinflammatory and anti-inflammatory cytokines, along with transcription of specific genes (1). Classically activated macrophages (M1) produce proinflammatory cytokines such as TNFα, IL-6 and IL-1β, and inducible nitric oxide synthase (iNOS) that will aid in the promotion of an anti-bacterial response, while alternatively activated macrophages (M2) accelerate the secretion of anti-inflammatory cytokines such as IL-10, and arginase-1 (Arg1), thus possessing immune suppressive roles (3, 4). Notably, although polarized macrophages can be categorized into these two main broad clusters with distinct phenotypes, a spectrum of polarization occurs in response to different environmental stimuli, and a plethora of transcription factors are involved in macrophage polarization in a temporally and spatially dependent manner (5, 6). Previous studies have defined the distinct role of certain transcription factors underlying macrophage polarization (7–10). For example, activation of interferon-regulatory factor (IRF) 5, NF-κB subunit p65, and signal transducer and activator of transcription (STAT) 1 promotes M1 polarization, while M2 polarization can be induced by a predominant expression of active STAT3 and STAT6 (7–10). However, the intracellular signaling pathways involved in macrophage polarization remain poorly defined, especially under the inflammatory milieu of many chronic infectious diseases.

Periodontitis is a polymicrobial infection-induced chronic inflammatory disease characterized by severe gingival inflammation and destruction of connective tissue surrounding the teeth. A growing body of evidence suggests that periodontitis may enhance the risk for several deadly conditions including cardiovascular diseases, diabetes, and some upper gastrointestinal cancers (11–14). The human oral cavity has various ecological niches such as the human gingival crevice and periodontal pocket and is inhabited by more than 700 species of bacterial species as well as other types of microorganisms (15). A plethora of virulence factors (i.e. capsule, LPS, fimbriae, proteinases) from oral microorganisms continuously stimulate host immune cells to initiate a wide range of inflammatory responses. A variety of immune cells including neutrophils, macrophages, monocytes, dendritic cells

and various lineages of T and B cells, have been shown to hierarchically orchestrate the immune-inflammatory responses in the gingival epithelium (16, 17). Although the function of neutrophils in oral inflammation has been widely investigated, the role of macrophages and their polarization under the periodontal inflammatory milieu has received less attention. Several recent studies have examined the relationship between macrophage polarization and periodontal disease status (18–21). The quantity of proinflammatory M1 macrophages is significantly increased in periodontitis tissues and the increase of M2 macrophages prevents ligation-induced bone loss in murine periodontitis models (20, 21). In contrast, a recent study reported that there is no substantial difference in macrophage polarization in the gingival tissues of periodontitis patients versus healthy controls (18). These controversial results suggest that more investigations are required to define macrophage polarization in inflamed gingival tissue and to elucidate the underlying regulatory mechanisms involved.

Serum- and glucocorticoid-inducible kinases (SGKs) are a class of serine/threonine kinases belonging to the AGC kinase family (Protein kinase A, -G and -C family) (22). There are three isoforms of SGK, namely SGK1, SGK2 and SGK3. SGK1 is widely expressed and rapidly responds to a variety of stimuli such as follicle stimulating hormone, osmotic shock, ischemia, transforming growth factor (TGF)-β, glucocorticoids and mineralocorticoids (22). Like Akt, SGK1 can be fully activated by phosphoinositide 3-kinase (PI3K) through phosphorylation at Thr256 by 3-phosphoinositide-dependent protein kinase (PDK)-1 and Ser422 by PDK2. Our previous studies have demonstrated that TLR-induced SGK1 restrains the intensity and duration of inflammation in an *E. coli* LPS-induced endotoxemia model (23). Moreover, SGK1 has been found to facilitate T helper type 2 cell differentiation by negatively regulating degradation of the transcription factor JunB (24). Recent studies have also reported that SGK1 deficiency or inhibition suppresses M2 macrophage polarization in angiotensin II-treated mouse cardiac tissue and in an experimental autoimmune encephalomyelitis model (25, 26). All of these findings suggest the anti-inflammatory role of SGK1 in immune-inflammatory responses. However, SGK1 was also reported to act as a pro-inflammatory regulator via promoting Th17 development, osteoclastogenesis, and enhancing pro-inflammatory cytokine production in other models (27–30). Therefore, the possible regulatory role of SGK1 on macrophage polarization in the inflammatory milieu is not well established, let alone the underlying molecular mechanisms.

In this study, we investigated the effect of SGK1 on macrophage polarization and revealed an undefined signaling pathway involved in using *LysM*-Cre-mediated SGK1-deficient mice. Moreover, we examined the effect of SGK1 on macrophage polarization and alveolar bone loss in a *Porphyromonas gingivalis* infection-induced periodontal inflammation model.

Materials and Methods

Mice and Reagents

LysM-Cre^{+} *sgk1*$^{fl/fl}$ mice were generated by crossing C57BL/6 mice possessing *LysM*-driven expression of Cre (from The Jackson Laboratory) to loxP flanked SGK1 mice (provided by Dr. Alexander; Dartmouth Medical School). The negative littermates from this breeding were used as controls. All the mice were housed in a specific-pathogen-free facility at Virginia Commonwealth University (VCU), and the VCU Institutional

Animal Care and Use Committee approved all animal protocols. All efforts were made to minimize the number of mice used and to prevent animal distress, pain, and injury. Carbon dioxide (CO_2) was used for euthanasia of mice. Ultrapure LPS from *E. coli 0111:B4* was from Invivogen (San Diego, CA). Phospho-SGK1 antibodies were from Santa Cruz Biotechnology. Total SGK1 antibodies were from Proteintech (Chicago, IL). Total iNOS and arginase1 antibodies were from EMD Millipore and BD Bioscience, respectively (Burlington, MA; Franklin Lakes, NJ). Anti-FoxO1 (S256) antibody was from Abcam (Cambridge, MA). All other antibodies were from Cell Signaling Technology (Danvers, MA). The SGK1 inhibitor EMD638683 was from MedChem Express (Monmouth Junction, NJ) and has been characterized and shown to be specific for SGK1 without discernible effects on a panel of 68 other kinases (31). All recombinant cytokines were from Peprotech (Rocky Hill, NJ). Non-targeting pools of siRNA and a mixture of four pre-validated siRNA duplexes specific for STAT3 (ON TARGET-*plus*™) were from GE-Healthcare Dharmacon (Pittsburgh, PA). All plasmids including STAT3- pcDNA3 (Cat. 8706) with Flag tag, pcDNA3 Flag HA (Cat. 10792) which was constructed with HA and Flag tags, were from Addgene (Watertown, MA). Mouse IL-12/IL-23 (p40) ELISA MAX™ Deluxe, Mouse IL-6, and Mouse TNFα cytokine ELISA kits were from Biolegend (San Diego, CA). RNeasy Mini and RNase-free DNase Set were from QIAGEN (Hilden, Germany). High Capacity cDNA reverse transcription kit and Taq-path qPCR master mix were from Applied Biosystem (Foster City, CA).

Preparation of BMDMs

Bone marrow-derived macrophages (BMDMs) were generated from femoral and tibial bone marrow cells as previously described (32). Briefly, bone marrow was flushed from the femur and tibiae of 8-week-old *LysM*-Cre$^+$ *sgk*$^{fl/fl}$ or the littermate control mice using sterile Hanks' balanced salt solution (Invitrogen, Carlsbad, CA) and homogenized by repeated passage through an 18.5-gauge needle. The cells were washed in PBS, centrifuged at 1500 rpm for 5 min, and resuspended in RPMI 1640 medium supplemented with 10% FBS (R10) (Invitrogen), 50 μM 2-mercaptoethanol, 1 mM sodium pyruvate, 2 mM L-glutamine, 20 mM HEPES, 50 units/ml penicillin, 50 μg/ml streptomycin, and 30% L929 culture supernatant. Nonadherent cells were collected after 24 h and cultured for 7 days in Costar ultra-low attachment polystyrene culture dishes with a medium change on day 4. On day 7, macrophages were about 95% F4/80$^+$/CD11b$^+$ as determined by flow cytometry and ready for further polarized stimulation with INFγ/LPS or IL-4/IL-13.

siRNA and plasmid transfection, cytokine assay, and western blots

For siRNA and plasmid transfections, BMDMs were transfected with nontargeting control siRNA, siRNA-SGK1, siRNA-STAT3, pcDNA3-STAT3, or pcDNA3 (empty vector control) using Lipofectamine RNAiMAX, or Lipofectamine LTX (Invitrogen, Carlsbad, CA) following the manufacturer's protocol. After transfection, the cells were directly seeded in either 96- or 6-well plates. After 48 hours, cells were treated with INFγ/LPS or IL-4/IL-13 for 24 h. The levels of total SGK1 and exogenous STAT3 were assessed by western blots. Cells were lysed in RIPA buffer containing phosphatase inhibitors for western blot assays. Images were acquired using the ImageQuant LAS 4100 (GE Healthcare Life Sciences, Pittsburg, PA). For cytokine assays, BMDMs were cultured in medium without

L929 culture supernatant for 24 hours. Cells were then either untreated (M0), treated with IFNγ (10ng/ml) and LPS (100 ng/mL) for M1 macrophages, or IL-4 (10ng/ml) and IL-13 (10ng/ml) for M2 macrophages. Culture supernatants were collected after 24 h stimulation. Cytokine concentrations were determined by enzyme-linked immunosorbent assay (ELISA) following the manufacturer's instructions.

RNA isolation and real-time quantitative PCR (qRT-PCR)

Total RNA was isolated using RNeasy ® Mini kit with RNase-Free DNase Set according to the manufacturer's instructions. RNA samples were reverse transcribed (RT) using a High Capacity cDNA reverse transcription kit. Real-time quantitative PCR analysis was performed using specific primers for mouse *sgk1* (Mm00441380), *Ym1 /Chil3* (Mm00657889_mH), *Mgl-1/ Clec10a* (Mm00546124), *Arg-1* (Mm00475988_m1), *iNOS* (Mm00440502_m1), *Fizz-1/Retnla* (Mm00445109), and *stat3* (Mm01219775_m1 (33) in an Applied Biosystems 7500 system using Taqpath qPCR master mix (Applied Biosystem). Relative levels of gene expression were determined using GAPDH (Mm99999915_g1) as the control (34).

Cell staining and Flow cytometry

BMDMs were either untreated or treated with IFNγ/LPS or IL-4/IL13 (10ng/ml, PeproTech) and were then washed twice with Flow Cytometry Staining Buffer and treated with Fc block for further flow cytometry assays. All the reagents below for flow cytometry assay are from eBioscience (San Dieago, CA). After washing and blocking, cells were incubated with the following fluorescently labeled anti-mouse antibodies: PerCP-cy5.5-conjugated F4/80 (45–4801-82); APC-conjugated CD11b (17–0112-81) or FITC-conjugated CD11b (11–0112-82); and PE-conjugated CD206 (12–2061-80), following the manufacturer's instructions. For intracellular staining, cells were fixed with IC Fixation Buffer for 30 min, followed by washing twice with permeabilization buffer and incubated with iNOS-APC (Thermofisher, Waltham, MA, #17–5920-80) for 30 mins. Stained cells were then washed and analyzed on LSRFortessa flow cytometer (BD Bioscience, US). Data were analyzed with the FlowJo software.

P. gingivalis-induced periodontal inflammation model and immunohistochemistry

Porphyromonas gingivalis 33277 was cultured anaerobically in trypticase soy broth supplemented with yeast extract (1 mg/ml), hemin (5 μg/ml) and menadione (1 μg/ml), and was grown at 37°C in Anoxomat jars (Spiral Biotech) under anaerobic conditions (10% H_2, 10% CO_2, 80% N_2, plus palladium catalyst). For the *P. gingivalis*-induced periodontal inflammation model, the endogenous oral microbiota was suppressed in 10- to 12-week-old C57/B6/J mice by sulfamethoxazole (800 μg/ml) and trimethoprim (400 μg/ml) provided *ad libitum* in water for 5 days. The mice then received pure drinking water for 5 days. Alveolar bone loss was induced by oral inoculation with 1×10^9 CFU of *P. gingivalis* suspended in 100 μl of phosphate-buffered saline with 2% carboxymethylcellulose. Inoculations were performed six times at two-day intervals. An experimental group was also intraperitoneally (IP) administered EMD638683 (15 mg/kg) with each inoculation and every other day thereafter until euthanization. The effect of EMD638683 on the growth of *P. gingivalis in vitro* was also assessed (Fig. S1A). Sham-infected and vehicle control mice were also

established. The mice were euthanized with CO_2 and cervical dislocation 42 days after the final infection. Maxillary gingiva from the upper half of each jaw was harvested for RT-PCR assay and the other half were for western blot assay. Fresh gingival tissues were immersed in RNAlater® (Ambion, Austin, TX. Cat. AM7020) or RIPA buffer with protease and phosphatase inhibitors (Millipore Sigma, Burlington, MA. Cat. P8340 and P0044) (1:100) and then stored at −20°C for further RT-PCR or western blot assay, respectively. The expression of inflammatory cytokines including TNFα, IL-6, and IL-12P40 were determined by real-time quantitative PCR (qPCR) using FastStart Universal SYBR Green Master (ROX) (Roche, Basel, Switzerland) according to the manufacturer's instructions. The primer sequences used for amplification are shown in supplemental figure 1 (Fig. S1B). Gene expression was normalized to the GAPDH exogenous control and measured using the ΔΔCT method as described in a previous study (35). Alveolar bone loss was measured in millimeters at 14 predetermined points on the maxillary molars of defleshed maxillae as the distance from the cement enamel junction (CEJ) to the alveolar bone crest (ABC). Bone loss was visualized by methylene blue/eosin staining and quantified using a Nikon SMX 800 dissecting microscope (40×) fitted with a Boeckeler VIA-170K video image marker measurement system. The results were expressed as the mean with S.D. The lower jaws of the mice were fixed in 4% paraformaldehyde, decalcified in immunocal solution (Statlab, Lewisville, TX) for 15 d and embedded in paraffin wax for immunohistochemistry assay. The paraffin-embedded tissue blocks were freshly cut into 4 μm mesiodistal sections for subsequent immunostaining with mouse CD68, CD163, CD206, and F4/80 antibodies, followed by secondary FITC or Alexa Fluor 350-conjugated antibodies. PBS containing normal rabbit serum was used as sham control. Images were captured using a fluorescence microscope (Nikon Elipse E800) and processed by Neurolucida. Tissue sections were also stained with STAT3 antibody with visualization using 3,3'-diaminobenzidine (DAB), and the images were captured using X-cite Fluorescence LED boost ZEISS microscope bright field with objective magnification of 20X and analyzed by counting positively stained cells using Image J software. ImageJ (NIH) analysis was performed as per the standard recommended algorithm (36). Images were imported and processed with color deconvolution, adjusted by threshold and measurement setting and get the percentage of positive staining areas.

Statistical analyses

The statistical significance of differences among groups was evaluated with the analysis of variance (ANOVA) and the Tukey multiple comparison test using the InStat program (GraphPad). Differences between groups were considered significant at the level of $P \leq 0.05$.

Results

SGK1 differentially regulates transcription of lineage-specific genes in macrophages

Our previous study has demonstrated that inhibition of SGK1 aggravates TLRs-mediated inflammatory responses (23). In order to explore the possible role of SGK1 in macrophage polarization, resting macrophages (M0) were treated with IFNγ/*E. coli* LPS to induce M1 or IL-4/IL-13 to induce M2 macrophage phenotypes. We first examined the response of SGK1 to the challenge of IFNγ/LPS or IL-4/13. We found stimulation with either IFNγ/LPS or IL-4/13 leads to the activation of SGK1, represented by the phosphorylation

of NDRG, a substrate of SGK1 in macrophages, indicating SGK1 might be involved in polarization of macrophage cells (Fig. 1A, B). We next utilized EMD638683, a specific pharmacological inhibitor of SGK1, to investigate the effect of SGK1 on the transcription of specific genes in macrophage polarization. The optimum concentration of EMD638683 was first determined by measuring its impact on phospho-NDRG and cell viability. We found that 10μM EMD638683 robustly enhances the production of LPS-induced TNFα (Fig. 1C) and reduces phosphorylation of NDRG1 (Fig. 1A) but does not cause substantial cell death after 24 h treatment (Fig. 1D). We therefore utilized 10μM EMD638683 throughout this study. Next, we found that inhibition of SGK1 leads to a significant increase of iNOS at mRNA and protein levels under M1 macrophage-inducing conditions (Fig. 1E, F), which was confirmed by flow cytometry analysis (Fig. 1H, I). In contrast, under M2 macrophage-inducing conditions, inhibition of SGK1 significantly reduces expression of arginase-1, resistin-like α (Retnla, Fizz1), chitinase-like protein 3(Chil3, Ym-1), and macrophage galactose-type C-type lectin 1(Mgl1) (Fig. 1J). We further confirmed the effect of SGK1 on the expression of arginase-1 by western blots (Fig. 1F). To account for possible differences in protocols for the *in vitro* differentiation of macrophages, we also utilized LPS only to polarize macrophages and tested the expression of iNOS. Similar trends of iNOS were also observed (data not shown) under the M1 macrophage-inducing conditions. In addition, we also examined the expression of CD206, a prototypical M2 macrophage molecular marker, and we found SGK1 inhibition significantly decreases expression of CD206 upon the treatment with IL4/IL-13 (Fig. 1K, L). Taken together, these results suggest that SGK1 differentially regulates the expression of sublineage-specific genes in M1 and M2 macrophages.

SGK1 suppresses production of M1 macrophage inflammatory cytokines and promotes IL-10 in M2 macrophages

Given the distinct inflammatory cytokines produced by M1 and M2 macrophages, we next investigated the possible regulatory role of SGK1 in the production of inflammatory cytokines. Our results showed that inhibition of SGK1 with EMD638683 significantly elevated TNFα, IL-6, and IL-12 at message and protein levels under M1 macrophage-inducing conditions (Fig. 2A to D). Notably, inhibition of SGK1 also reduced IL-10 at the message level under M2 macrophage priming conditions (Fig. 2E). To avoid the possible non-specific effects of the chemical inhibitor, we utilized pre-validated siRNA to silence SGK1 (Fig. 2F, G) and we found that SGK1 silencing enhances production of pro-inflammatory cytokines (TNFα, IL-6, and IL-12) under M1 macrophage inducing conditions (Fig. 2H to J). Moreover, silencing of SGK1 also leads to a significant increase in iNOS expression (Fig. 2K) and decrease in arginase-1(Fig. 2L). This is consistent with our results using SGK1 inhibitor and consolidates the effect of SGK1 on macrophage differentiation. The distinct effects of SGK1 on the production of M1 and M2 inflammatory cytokines and sublineage-specific genes suggest that SGK1 suppresses M1 but promotes M2 phenotypes and thus regulates macrophage polarization.

Myeloid lineage-specific deletion of *sgk1* promotes macrophage polarization to M1 phenotype

To avoid the possible off-target effects of *sgk1* siRNA, we next used *sgk1* deficient BMDMs from *LysM*-Cre^{+} *sgk1*$^{fl/fl}$ mice, which were generated in our lab by crossing *LysM*-Cre^{+} mice with *sgk1*$^{loxp/loxp}$ mice and exhibit loss of *sgk1* gene in BMDMs (Fig. S2A). As expected, phosphorylation of NDRG was abrogated in macrophages from *LysM*-Cre^{+} sgk1$^{fl/fl}$ mice, suggesting SGK1 protein was expunged in bone marrow derived macrophages (Fig. 3A; Fig. S2A). Using BMDMs from *LysM*-Cre^{+} sgk1$^{fl/fl}$ mice we found that SGK1 deficiency leads to a significant increase of iNOS at message levels under M1 macrophage priming conditions (Fig. 3B). The results were further confirmed by western blots and flow cytometry assay (Fig. 3C to E). Moreover, compared to the littermate control, SGK1-deficient macrophages produced significantly higher amount of pro-inflammatory cytokines including TNFα, IL-12 and IL-6 at message and protein levels (Fig. 3F to H). On the other hand, SGK1-deficient macrophages produced significantly lower levels of arginase-1 and two other M2 macrophage specific genes, Fizz1 and Ym1 as compare to the littermate control under the M2 macrophage priming conditions (Fig. 3I). The expression of arginiase-1 was also confirmed by western blots (Fig. 3J and K). Taken together, these results suggested that SGK1 can indeed suppress expression of M1 while promoting M2 phenotypes in the process of macrophages polarization.

SGK1 differentially regulates expression of FoxO1 and STAT3 in macrophages

Previous studies have demonstrated that there are a plethora of transcription factors comprehensively controlling macrophage polarization, such as M1-promoting transcription factors NF-κB, STAT1, and IRF5, and M2-promoting transcription factors IRF4, PPARγ, STAT3 and STAT6 (2, 9). We next investigated the effect of SGK1 deletion on the activity of prototypical transcription factors in macrophage polarization. Using *LysM*-mediated *sgk1* deficient macrophages from the mice described above, we found there was a slight increase of NF-κB but we did not observe substantial changes of STAT1, IRF5, or PPARγ in *sgk1*$^{-/-}$ macrophages as compared to the littermate control macrophages under M1 macrophage priming conditions (Data not shown). Surprisingly, the expression of FoxO1 was remarkably higher in *sgk1*$^{-/-}$ macrophages than in littermate control macrophages (Fig. 4A). Moreover, SGK1 deficiency led to a decrease of FoxO1 phosphorylation under M1 macrophage-inducing conditions (Fig. 4A). Since the decreased phosphorylation of FoxO1 has been demonstrated to result in sequestration of FoxO1 in the nucleus and to enhance its activity (17, 37), we next to investigated if SGK1 deficiency can suppresses cytoplasmic translocation of FoxO1, sequester it in the nucleus and thus enhance its activity. As shown in figure 4B and C, while cytosolic FoxO1 in macrophages from normal littermates continuously increased after 6- and 24- hours stimulation with LPS/IFNγ, the nuclear FoxO1 concurrently decreased during this time (Fig. 4B), indicating FoxO1 indeed translocated from the nucleus to the cytoplasm. However, in macrophages from *sgk1−/−* mice, FoxO1 translocation to the cytoplasm was abrogated, which resulted in relatively more FoxO1 in the nucleus (Fig. 4C). These results are consistent with our and other previous studies (17, 38–40) showing that cytoplasmic translocation of FoxO1 is a key anti-inflammatory mechanism to restrain LPS-induced inflammatory responses. On the other hand, we found that SGK1 deficiency decreases STAT3 expression and phosphorylation

under M2 macrophage-inducing conditions (Fig. 4D), which is also consistent with previous studies showing that SGK1 regulates NF-κB and STAT3 under different contexts (23, 25). Interestingly, no substantial differences were observed in the expression and activity of STAT6, a prototypical transcription factor driving macrophage polarization toward M2 phenotypes (Fig. 4D). Taken together, our results demonstrated that SGK1 can modulate the phosphorylation and expression of FoxO1 and STAT3 in macrophages under different polarization conditions.

FoxO1 and STAT3 regulates expression of lineage-specific macrophage genes

Given that SGK1 deficiency leads to a remarkable alteration of FoxO1 and STAT3, we next investigated if FoxO1 and STAT3 affected the phenotypes of M1 and M2 macrophages, respectively. We found that inhibition of FoxO1 with a specific chemical inhibitor, AS1842856, indeed decreased SGK1 deficiency-enhanced iNOS (Fig. 5A), as well as TNFα, IL-6 and IL-12P40 under M1 inducing conditions (Fig. 5B to D). Moreover, silencing of STAT3 by pre-validated siRNAs (Fig. 5E) significantly diminished transcription of M2 specific genes, arginase-1, Fizz1, and Ym1 (Fig. 5F), as well as IL-10 (Fig. 5G) under M2 inducing conditions. In addition, a plasmid encoding exogenous STAT3 was used to exclude the possible off-target effects of the siRNA and confirm the role of STAT3 in M2 macrophage polarization (Fig. 5H). We found that compared with control macrophages, STAT3-overexpressing macrophages had a remarkably increased in expression of arginase 1 (Fig. 5H), and significantly higher levels of Fizz1 and Ym1 transcripts (Fig. 5I) under M2 macrophage priming conditions. Taken together, these results clearly show that FoxO1 and STAT3 are involved in SGK1-mediated M1 and M2 macrophage polarization, respectively.

SGK1 promotes M2 macrophage polarization and protects against alveolar bone loss in *P. gingivalis*-infected mice

A *P. gingivalis*-induced murine periodontal inflammation model has been widely used in periodontitis research. Inflamed gingival tissue is often densely colonized with microorganisms and infiltrated with various inflammatory cytokines such as IFNγ, IL-4, and IL-13, which forms a niche for macrophage polarization (41–43). Previous studies have shown that *P. gingivalis* infection leads to inflammatory responses through activation of TLR2 and/or TLR4 on the surface of immune cells (44–46). To further investigate the potential effects of SGK1 on macrophage phenotypes in *P. gingivalis*-infected gingival tissues, we first examined the expression of putative macrophage markers, CD68 and F4/F80, and the prototypical M2 molecular markers, CD163 and CD206. As shown in figure 6A to C, infection of *P. gingivalis* led to an increase of total macrophages in gingival tissues, represented by the enhanced expression of CD68 and F4/F80 (Fig. 6A and B). Interestingly, mice pretreated with SGK1 inhibitor demonstrated significantly lower expression of CD206 and CD163 than the mice treated with *P. gingivalis* only (Fig. 6A and C). On the other hand, we observed that mice pretreated with the SGK1 inhibitor produced significantly higher amounts of IL-6 mRNA and protein as compared to the mice treated with *P. gingivalis* only (Fig. 6D, E). However, there were no substantial differences observed at the mRNA and protein levels for TNFα or IL-12P40 (Fig. 6E). This discrepancy between *in vitro* and *in vivo* responses to SGK1 inhibition may be due to the phase of inflammation, differential dynamics of cytokines synthesis, and importantly, the different

sampling of cells, indicating that complicated regulatory mechanisms are involved in the progression of chronic inflammation. In addition, we also examined whether SGK1 affects inflammation-mediated alveolar bone loss, which is a characteristic of *P. gingivalis*-induced periodontitis. As shown in figure 6 F and G, *P. gingivalis* infection induced a significant bone loss, and inhibition of SGK1 significantly aggravated the severity of the bone loss as determined through the measurement of the cementoenamel junction (CEJ)- alveolar bone crest (ABC) distance (Fig. 6F, G). Taken together, these findings suggest that SGK1 restrains periodontal inflammation through facilitating M2 macrophage polarization and curtailment of M1 polarization, and protects against oral bone loss in *P. gingivalis*-infected mice.

SGK1 regulates expression of STAT3 in mouse gingival tissues

Given that we have demonstrated STAT3 as a key transcription factor involved in SGK1-mediated macrophage polarization in a cell culture model, we next examined if SGK1 inhibition affected expression of STAT3 in *P. gingivalis*-infected mouse gingival tissues. As shown in figure 7, compared with the sham control mice, *P. gingivalis* infected mice had a significantly higher level of STAT3 in gingival tissues (Fig. 7A, C), which is consistent with our results showing that *P. gingivalis* infection enhances the expression of M2 macrophage molecular markers (Fig. 6A). However, inhibition of SGK1 using a chemical inhibitor, EMD638683, led to a significant decrease of STAT3 in *P. gingivalis* infected mouse gingival tissues, as compared to the sham control mice or mice treated with EMD638683 only (Fig. 7A, C). These results suggest that SGK1 is necessary to maintain expression of STAT3, through which it promotes macrophage polarization to M2 phenotypes.

Discussion

Plasticity and polarization of macrophages are key to immune responses during inflammation. In this study, we investigated whether SGK1 is involved in macrophage polarization. We have demonstrated that SGK1 is indeed a major factor in defining macrophage polarization. Inhibition of SGK1 increases characteristic gene-expression of M1 macrophages and enhances pro-inflammatory cytokine production in BMDMs. Moreover, deficiency of SGK1 leads to less secretion of IL-10 and reduces M2-specific gene expression, indicating SGK1 is essential for maintenance of alternative macrophages. We also found that SGK1 suppresses M1- but promotes M2- macrophage polarization and protects against alveolar bone loss in *P. gingivalis*-infected mice. In addition, we demonstrated that FoxO1 and STAT3 are regulated by SGK1 and drive macrophage polarization to M1 and M2, respectively. Therefore, SGK1 is key for macrophage plasticity and function, which could be an interventional target to manipulate the polarization of macrophages and conversion of one subset of macrophages to the other (Fig. 8).

Many transcription factors are involved in immune-inflammatory responses of macrophages to various environment stimuli. In this study, while the function of SGK1-mediated activation of FoxO1 and STAT3 in macrophage polarization was demonstrated, we also found that SGK1 inhibition or deficiency slightly enhances expression of NF-κBp65 (data not shown). Thus, we can't exclude the possibility that NF-κBp65 is also partially involved in macrophage polarization, although it may not be a major player. On the other hand, Akt

signaling is similar to SGK1 and has been reported to be key in macrophage polarization (47–49). Therefore, it is possible that the compensation of SGK1 signaling by Akt may impact macrophage polarization in our models. However, we did not observe any significant changes for Akt phosphorylation (data not shown), indicating SGK1 could be a non-redundant regulator in the process of macrophage polarization. Thus, our results indicated that combinatorial expression of various transcription factors and hierarchical activation (or repression) could be a paradigm to specify macrophage phenotype and thus direct macrophage polarization. Further investigations of the contribution of specific transcription factors to macrophage polarization and their interactions are warranted to characterize SGK1-mediated signaling and subsequent application for the control of inflammatory diseases.

A delicate balance between pro- and anti- inflammatory mechanisms is critical in the oral mucosa immune system to effectively protect against microbial invasion and avoid excessive inflammation. Our previous study has demonstrated that SGK1 plays an essential role in the suppression of TLR-mediated inflammatory responses (23). In this study, we have found that the expression of both M1 macrophage and M2 macrophage markers are increased in *P. gingivalis*-infected mice model. Given that both *E. coli* LPS and IL-4/IL-13 can phospho-activate SGK1, it is possible that activation of SGK1 upon various external stimuli acts as a rheostat that fine-tunes inflammatory cytokine production and macrophage polarization to maintain the homeostasis of inflammatory responses. On the other hand, our results also showed that *P. gingivalis* infection leads to phospho-activation of SGK1 in BMDMs (Fig. S2B), indicating *P. gingivalis* may facilitate macrophage polarization toward M2 phenotypes through manipulating SGK1 activity, which is consistent with the results from a previous study showing that *P. gingivalis* is a weak inducer for macrophage polarization (50). A very recent study validated this point by showing that *P. gingivalis* infection indeed promotes M2 macrophage polarization and facilitates immunoevasion of oral cancer cells (51). Given that macrophage polarization represents a spectrum of states through which cells can transition in either direction (2), the interaction between *P. gingivalis* infection and activation of SGK1 suggests a pivotal interventional role for SGK1 signaling in the control of macrophage polarization. Therefore, a possible paradigm is that bacterial infection may result in the recruitment of additional macrophages to local inflammatory sites where specific signaling is responsible for finetuning of macrophage polarization to pro- or anti-inflammatory sublineages. Thus, the SGK1-mediated bifurcated signaling pathway could be a key signaling axis exploited by *P. gingivalis* to manipulate macrophage polarization and benefit its survival in the periodontal inflammatory milieu.

In this study, our results have shown a discrepancy in different inflammatory cytokine production in *in vitro* versus *in vivo* assays. SGK1 inhibition significantly enhanced the production of IL-6, IL-12, and TNFα in cultured cells, while only IL-6 was significantly increased in the gingival tissue from *P. gingivalis*-infected mice. This discrepancy might be caused by multiple factors including the phase of inflammation, variant resistance to *P. gingivalis*-induced tolerance, and importantly, the different components of samples. In our animal model, the gingival tissues for TNFα and IL-12 analysis were from mice infected with *P. gingivalis* for 42 days, which is approximately equal to 6 years' infection in humans. Compared to the cultured cells challenged with IFNγ and LPS for only 24 hours, it would

not be surprising to see different levels of TNFα and IL-12 resulting from the different phases of inflammation in the two systems. Moreover, previous studies have shown that TNFα and IL-12 are more prone to chronic activation-mediated immune cell tolerance than IL-6 (52, 53). Since the mice in our model were infected with *P. gingivalis* for 12 days, it is also reasonable to speculate that immune cell tolerance in gingival tissue could obscure the effect of SGK1 on TNFα and IL-12 expression. In addition, differences of the samples we used *in vitro* and *in vivo* could also be a major reason for this discrepancy. Unlike *in vitro* cultured macrophages, gingival tissue includes not only macrophages, but also monocytes, neutrophils, adaptive immune cells, epithelial cells, fibroblasts and other cells. The different regulatory functions of SGK1 in innate and adaptive immune cells, which has been extensively reported (27, 54), may counterbalance SGK1-mediated enhancement of TNFα and IL-12 production in macrophages. Due to the limited size of murine gingival tissue, it is difficult to isolate sufficient monocytes, macrophages, or adaptive immune cells to test the possible distinct functions of SGK1 in each. Future research focusing on the expression of polarization molecular markers and production of inflammatory cytokines at different phases of *P. gingivalis* infection, and the use of single-cell sequencing from pooled tissues or cervical lymph nodes may allow for a rigorous test of this hypothesis.

In this study, we found that SGK1 deficiency leads to an increase in FoxO1 and a decrease in STAT3 in macrophages under M1 and M2 priming conditions, respectively. However, we have not demonstrated how SGK1 deficiency regulates expression of FoxO1 and STAT3 in macrophages. While our supplemental data (Fig. S2C) showed that SGK1 deficiency enhances the mRNA levels of FoxO1, suggesting SGK1 may impact the *de novo* synthesis of FoxO1, it is still not clear why the expression of STAT3 was reduced in *sgk1* deficient BMDMs. Previous studies have shown that SGK1 activation could phosphorylate Nedd4–2 (55), a member of HECT family of ubiquitin E3 ligases, and thereby reduce its activity, which would lessen the amount of ubiquitin transferred to the substrate. Thus, it is possible that SGK1 deficiency in macrophages reduces phosphorylation of Nedd4–2, enhances its activity, promotes ubiquitination-mediated degradation of STAT3, and ultimately decreases STAT3 levels. Combined with the decreased phosphorylation of STAT3, deficiency of SGK1 could substantially reduce STAT3 activity and suppresses M2 macrophage polarization. While the decreased phosphorylation of STAT3 possibly results from the diminished total STAT3 levels in SGK1 knockout cells, we can't exclude the potential influences of autocrine signaling, such as STAT3-mediated IL-10, on STAT3 phosphorylation. It is likely that diminished STAT3 may suppress IL-10 transcription (56), which is a strong inducer of STAT3 phosphorylation (57), and thereby reduce STAT3 phosphorylation in M2-primed macrophages. Thus, SGK1-regulated expression of STAT3 and FoxO1 could be through different mechanisms. Further investigation of this point is likely to yield greater insight into macrophage polarization in general.

In summary, we have demonstrated for the first time that SGK1 is necessary for the maintenance of M2 macrophages and protects against *P. gingivalis*-induced alveolar bone loss in a mouse model of periodontitis. SGK1 inhibition promotes M1 polarization and restrains M2 macrophage phenotypes are through the control of FoxO1 and STAT3, respectively. Combined with our previous study showing that SGK1 restrains TLR-mediated

inflammation, our findings suggest that SGK1 could be an important interventional target for manipulating the magnitude and duration of inflammation depending on clinical necessity.

Supplementary Material

Refer to Web version on PubMed Central for supplementary material.

Acknowledgments

We thank Dr. Todd Kitten for critical reading of the manuscript.

Funding Sources

This research was supported by Grant DE026727 (H.W.) from the U.S. National Institutes of Health, National Institute of Dental and Craniofacial Research.

References

1. Chen S, Yang J, Wei Y, and Wei X. 2020. Epigenetic regulation of macrophages: from homeostasis maintenance to host defense. Cell Mol Immunol 17: 36–49. [PubMed: 31664225]
2. Murray PJ 2017. Macrophage Polarization. Annu Rev Physiol 79: 541–566. [PubMed: 27813830]
3. Orecchioni M, Ghosheh Y, Pramod AB, and Ley K. 2019. Macrophage Polarization: Different Gene Signatures in M1(LPS+) vs. Classically and M2(LPS-) vs. Alternatively Activated Macrophages. Front Immunol 10: 1084. [PubMed: 31178859]
4. Glass CK, and Natoli G. 2016. Molecular control of activation and priming in macrophages. Nat Immunol 17: 26–33. [PubMed: 26681459]
5. Zhou D, Huang C, Lin Z, Zhan S, Kong L, Fang C, and Li J. 2014. Macrophage polarization and function with emphasis on the evolving roles of coordinated regulation of cellular signaling pathways. Cell Signal 26: 192–197. [PubMed: 24219909]
6. Hume DA 2015. The Many Alternative Faces of Macrophage Activation. Front Immunol 6: 370. [PubMed: 26257737]
7. Degboe Y, Rauwel B, Baron M, Boyer JF, Ruyssen-Witrand A, Constantin A, and Davignon JL 2019. Polarization of Rheumatoid Macrophages by TNF Targeting Through an IL-10/STAT3 Mechanism. Front Immunol 10: 3. [PubMed: 30713533]
8. Kapoor N, Niu J, Saad Y, Kumar S, Sirakova T, Becerra E, Li X, and Kolattukudy PE 2015. Transcription factors STAT6 and KLF4 implement macrophage polarization via the dual catalytic powers of MCPIP. J Immunol 194: 6011–6023. [PubMed: 25934862]
9. Krausgruber T, Blazek K, Smallie T, Alzabin S, Lockstone H, Sahgal N, Hussell T, Feldmann M, and Udalova IA 2011. IRF5 promotes inflammatory macrophage polarization and TH1-TH17 responses. Nat Immunol 12: 231–238. [PubMed: 21240265]
10. Schultze JL, and Schmidt SV 2015. Molecular features of macrophage activation. Semin Immunol 27: 416–423. [PubMed: 27049460]
11. Gao S, Li S, Ma Z, Liang S, Shan T, Zhang M, Zhu X, Zhang P, Liu G, Zhou F, Yuan X, Jia R, Potempa J, Scott DA, Lamont RJ, Wang H, and Feng X. 2016. Presence of Porphyromonas gingivalis in esophagus and its association with the clinicopathological characteristics and survival in patients with esophageal cancer. Infect Agent Cancer 11: 3. [PubMed: 26788120]
12. Olsen I, Taubman MA, and Singhrao SK 2016. Porphyromonas gingivalis suppresses adaptive immunity in periodontitis, atherosclerosis, and Alzheimer's disease. J Oral Microbiol 8: 33029. [PubMed: 27882863]
13. Olsen I, and Yilmaz O. 2016. Modulation of inflammasome activity by Porphyromonas gingivalis in periodontitis and associated systemic diseases. J Oral Microbiol 8: 30385. [PubMed: 26850450]
14. Dominy SS, Lynch C, Ermini F, Benedyk M, Marczyk A, Konradi A, Nguyen M, Haditsch U, Raha D, Griffin C, Holsinger LJ, Arastu-Kapur S, Kaba S, Lee A, Ryder MI, Potempa B, Mydel P, Hellvard A, Adamowicz K, Hasturk H, Walker GD, Reynolds EC, Faull RLM, Curtis MA,

Dragunow M, and Potempa J. 2019. Porphyromonas gingivalis in Alzheimer's disease brains: Evidence for disease causation and treatment with small-molecule inhibitors. Sci Adv 5: eaau3333. [PubMed: 30746447]

15. Parahitiyawa NB, Scully C, Leung WK, Yam WC, Jin LJ, and Samaranayake LP 2010. Exploring the oral bacterial flora: current status and future directions. Oral Dis 16: 136–145. [PubMed: 19627515]
16. Ebersole JL, Kirakodu SS, Novak MJ, Orraca L, Martinez JG, Cunningham LL, Thomas MV, Stromberg A, Pandruvada SN, and Gonzalez OA 2016. Transcriptome Analysis of B Cell Immune Functions in Periodontitis: Mucosal Tissue Responses to the Oral Microbiome in Aging. Front Immunol 7: 272. [PubMed: 27486459]
17. Graves DT, and Milovanova TN 2019. Mucosal Immunity and the FOXO1 Transcription Factors. Front Immunol 10: 2530. [PubMed: 31849924]
18. Garaicoa-Pazmino C, Fretwurst T, Squarize CH, Berglundh T, Giannobile WV, Larsson L, and Castilho RM 2019. Characterization of macrophage polarization in periodontal disease. J Clin Periodontol 46: 830–839. [PubMed: 31152604]
19. Gonzalez OA, Novak MJ, Kirakodu S, Stromberg A, Nagarajan R, Huang CB, Chen KC, Orraca L, Martinez-Gonzalez J, and Ebersole JL 2015. Differential Gene Expression Profiles Reflecting Macrophage Polarization in Aging and Periodontitis Gingival Tissues. Immunol Invest 44: 643–664. [PubMed: 26397131]
20. Zhou LN, Bi CS, Gao LN, An Y, Chen F, and Chen FM 2019. Macrophage polarization in human gingival tissue in response to periodontal disease. Oral Dis 25: 265–273. [PubMed: 30285304]
21. Zhuang Z, Yoshizawa-Smith S, Glowacki A, Maltos K, Pacheco C, Shehabeldin M, Mulkeen M, Myers N, Chong R, Verdelis K, Garlet GP, Little S, and Sfeir C. 2019. Induction of M2 Macrophages Prevents Bone Loss in Murine Periodontitis Models. J Dent Res 98: 200–208. [PubMed: 30392438]
22. Tessier M, and Woodgett JR 2006. Serum and glucocorticoid-regulated protein kinases: variations on a theme. J Cell Biochem 98: 1391–1407. [PubMed: 16619268]
23. Zhou H, Gao S, Duan X, Liang S, Scott DA, Lamont RJ, and Wang H. 2015. Inhibition of serum- and glucocorticoid-inducible kinase 1 enhances TLR-mediated inflammation and promotes endotoxin-driven organ failure. FASEB J 29: 3737–3749. [PubMed: 25993992]
24. Heikamp EB, Patel CH, Collins S, Waickman A, Oh MH, Sun IH, Illei P, Sharma A, Naray-Fejes-Toth A, Fejes-Toth G, Misra-Sen J, Horton MR, and Powell JD 2014. The AGC kinase SGK1 regulates TH1 and TH2 differentiation downstream of the mTORC2 complex. Nat Immunol 15: 457–464. [PubMed: 24705297]
25. Yang M, Zheng J, Miao Y, Wang Y, Cui W, Guo J, Qiu S, Han Y, Jia L, Li H, Cheng J, and Du J. 2012. Serum-glucocorticoid regulated kinase 1 regulates alternatively activated macrophage polarization contributing to angiotensin II-induced inflammation and cardiac fibrosis. Arterioscler Thromb Vasc Biol 32: 1675–1686. [PubMed: 22556335]
26. Li B, Tan TB, Wang L, Zhao XY, and Tan GJ 2019. p38MAPK/SGK1 signaling regulates macrophage polarization in experimental autoimmune encephalomyelitis. Aging (Albany NY) 11: 898–907. [PubMed: 30716717]
27. Gan W, Ren J, Li T, Lv S, Li C, Liu Z, and Yang M. 2018. The SGK1 inhibitor EMD638683, prevents Angiotensin II-induced cardiac inflammation and fibrosis by blocking NLRP3 inflammasome activation. Biochim Biophys Acta Mol Basis Dis 1864: 1–10. [PubMed: 28986310]
28. Xi X, Zhang J, Wang J, Chen Y, Zhang W, Zhang X, Du J, and Zhu G. 2019. SGK1 Mediates Hypoxic Pulmonary Hypertension through Promoting Macrophage Infiltration and Activation. Anal Cell Pathol (Amst) 2019: 3013765. [PubMed: 31815093]
29. Zhang Z, Xu Q, Song C, Mi B, Zhang H, Kang H, Liu H, Sun Y, Wang J, Lei Z, Guan H, and Li F. 2020. Serum- and Glucocorticoid-inducible Kinase 1 is Essential for Osteoclastogenesis and Promotes Breast Cancer Bone Metastasis. Mol Cancer Ther 19: 650–660. [PubMed: 31694887]
30. Kleinewietfeld M, Manzel A, Titze J, Kvakan H, Yosef N, Linker RA, Muller DN, and Hafler DA 2013. Sodium chloride drives autoimmune disease by the induction of pathogenic TH17 cells. Nature 496: 518–522. [PubMed: 23467095]

31. Ackermann TF, Boini KM, Beier N, Scholz W, Fuchss T, and Lang F. 2011. EMD638683, a novel SGK inhibitor with antihypertensive potency. Cell Physiol Biochem 28: 137–146. [PubMed: 21865856]
32. Weischenfeldt J, and Porse B. 2008. Bone Marrow-Derived Macrophages (BMM): Isolation and Applications. CSH Protoc 2008: pdb prot5080.
33. Byles V, Covarrubias AJ, Ben-Sahra I, Lamming DW, Sabatini DM, Manning BD, and Horng T. 2013. The TSC-mTOR pathway regulates macrophage polarization. Nat Commun 4: 2834. [PubMed: 24280772]
34. Kirkby NS, Chan MV, Zaiss AK, Garcia-Vaz E, Jiao J, Berglund LM, Verdu EF, Ahmetaj-Shala B, Wallace JL, Herschman HR, Gomez MF, and Mitchell JA 2016. Systematic study of constitutive cyclooxygenase-2 expression: Role of NF-kappaB and NFAT transcriptional pathways. Proc Natl Acad Sci U S A 113: 434–439. [PubMed: 26712011]
35. Wang H, Garcia CA, Rehani K, Cekic C, Alard P, Kinane DF, Mitchell T, and Martin M. 2008. IFN-beta production by TLR4-stimulated innate immune cells is negatively regulated by GSK3-beta. J Immunol 181: 6797–6802. [PubMed: 18981097]
36. Crowe AR, and Yue W. 2019. Semi-quantitative Determination of Protein Expression using Immunohistochemistry Staining and Analysis: An Integrated Protocol. Bio Protoc 9.
37. Wallerstedt E, Sandqvist M, Smith U, and Andersson CX 2011. Anti-inflammatory effect of insulin in the human hepatoma cell line HepG2 involves decreased transcription of IL-6 target genes and nuclear exclusion of FOXO1. Mol Cell Biochem 352: 47–55. [PubMed: 21298325]
38. Brown J, Wang H, Suttles J, Graves DT, and Martin M. 2011. Mammalian target of rapamycin complex 2 (mTORC2) negatively regulates Toll-like receptor 4-mediated inflammatory response via FoxO1. J Biol Chem 286: 44295–44305. [PubMed: 22045807]
39. Li B, Lei J, Yang L, Gao C, Dang E, Cao T, Xue K, Zhuang Y, Shao S, Zhi D, Hao J, Jin L, Qiao P, Ouyang W, and Wang G. 2019. Dysregulation of Akt-FOXO1 Pathway Leads to Dysfunction of Regulatory T Cells in Patients with Psoriasis. J Invest Dermatol 139: 2098–2107. [PubMed: 30998985]
40. Liu F, Qiu H, Xue M, Zhang S, Zhang X, Xu J, Chen J, Yang Y, and Xie J. 2019. MSC-secreted TGF-beta regulates lipopolysaccharide-stimulated macrophage M2-like polarization via the Akt/FoxO1 pathway. Stem Cell Res Ther 10: 345. [PubMed: 31771622]
41. Pan W, Wang Q, and Chen Q. 2019. The cytokine network involved in the host immune response to periodontitis. Int J Oral Sci 11: 30. [PubMed: 31685798]
42. Stadler AF, Angst PD, Arce RM, Gomes SC, Oppermann RV, and Susin C. 2016. Gingival crevicular fluid levels of cytokines/chemokines in chronic periodontitis: a meta-analysis. J Clin Periodontol 43: 727–745. [PubMed: 27027257]
43. Cekici A, Kantarci A, Hasturk H, and Van Dyke TE 2014. Inflammatory and immune pathways in the pathogenesis of periodontal disease. Periodontol 2000 64: 57–80. [PubMed: 24320956]
44. Darveau RP, Pham TT, Lemley K, Reife RA, Bainbridge BW, Coats SR, Howald WN, Way SS, and Hajjar AM 2004. Porphyromonas gingivalis lipopolysaccharide contains multiple lipid A species that functionally interact with both toll-like receptors 2 and 4. Infect Immun 72: 5041–5051. [PubMed: 15321997]
45. Burns E, Bachrach G, Shapira L, and Nussbaum G. 2006. Cutting Edge: TLR2 is required for the innate response to Porphyromonas gingivalis: activation leads to bacterial persistence and TLR2 deficiency attenuates induced alveolar bone resorption. J Immunol 177: 8296–8300. [PubMed: 17142724]
46. Nativel B, Couret D, Giraud P, Meilhac O, d'Hellencourt CL, Viranaicken W, and Da Silva CR 2017. Porphyromonas gingivalis lipopolysaccharides act exclusively through TLR4 with a resilience between mouse and human. Sci Rep 7: 15789. [PubMed: 29150625]
47. Luyendyk JP, Schabbauer GA, Tencati M, Holscher T, Pawlinski R, and Mackman N. 2008. Genetic analysis of the role of the PI3K-Akt pathway in lipopolysaccharide-induced cytokine and tissue factor gene expression in monocytes/macrophages. J Immunol 180: 4218–4226. [PubMed: 18322234]

48. Vergadi E, Ieronymaki E, Lyroni K, Vaporidi K, and Tsatsanis C. 2017. Akt Signaling Pathway in Macrophage Activation and M1/M2 Polarization. J Immunol 198: 1006–1014. [PubMed: 28115590]

49. Arranz A, Doxaki C, Vergadi E, Martinez Y. de la Torre, Vaporidi K, Lagoudaki ED, Ieronymaki E, Androulidaki A, Venihaki M, Margioris AN, Stathopoulos EN, Tsichlis PN, and Tsatsanis C. 2012. Akt1 and Akt2 protein kinases differentially contribute to macrophage polarization. Proc Natl Acad Sci U S A 109: 9517–9522. [PubMed: 22647600]

50. Lam RS, O'Brien-Simpson NM, Holden JA, Lenzo JC, Fong SB, and Reynolds EC 2016. Unprimed, M1 and M2 Macrophages Differentially Interact with Porphyromonas gingivalis. PLoS One 11: e0158629. [PubMed: 27383471]

51. Liu S, Zhou X, Peng X, Li M, Ren B, Cheng G, and Cheng L. 2020. Porphyromonas gingivalis Promotes Immunoevasion of Oral Cancer by Protecting Cancer from Macrophage Attack. J Immunol 205: 282–289. [PubMed: 32471882]

52. Natarajan S, Kim J, and Remick DG 2008. Acute pulmonary lipopolysaccharide tolerance decreases TNF-alpha without reducing neutrophil recruitment. J Immunol 181: 8402–8408. [PubMed: 19050257]

53. Wittmann M, Larsson VA, Schmidt P, Begemann G, Kapp A, and Werfel T. 1999. Suppression of interleukin-12 production by human monocytes after preincubation with lipopolysaccharide. Blood 94: 1717–1726. [PubMed: 10477697]

54. Wu C, Yosef N, Thalhamer T, Zhu C, Xiao S, Kishi Y, Regev A, and Kuchroo VK 2013. Induction of pathogenic TH17 cells by inducible salt-sensing kinase SGK1. Nature 496: 513–517. [PubMed: 23467085]

55. Caohuy H, Yang Q, Eudy Y, Ha TA, Xu AE, Glover M, Frizzell RA, Jozwik C, and Pollard HB 2014. Activation of 3-phosphoinositide-dependent kinase 1 (PDK1) and serum- and glucocorticoid-induced protein kinase 1 (SGK1) by short-chain sphingolipid C4-ceramide rescues the trafficking defect of DeltaF508-cystic fibrosis transmembrane conductance regulator (DeltaF508-CFTR). J Biol Chem 289: 35953–35968. [PubMed: 25384981]

56. Fu W, Hu W, Shi L, Mundra JJ, Xiao G, Dustin ML, and Liu CJ 2017. Foxo4- and Stat3-dependent IL-10 production by progranulin in regulatory T cells restrains inflammatory arthritis. FASEB J 31: 1354–1367. [PubMed: 28011648]

57. Finbloom DS, and Winestock KD 1995. IL-10 induces the tyrosine phosphorylation of tyk2 and Jak1 and the differential assembly of STAT1 alpha and STAT3 complexes in human T cells and monocytes. J Immunol 155: 1079–1090. [PubMed: 7543512]

Key points

- SGK1 promotes alternative, while suppressing inflammatory, macrophage polarization;
- SGK1 inversely regulates FoxO1 and STAT3 to control macrophage phenotypes;
- SGK1 protects against *P. gingivalis*-induced periodontal bone loss in a mouse model.

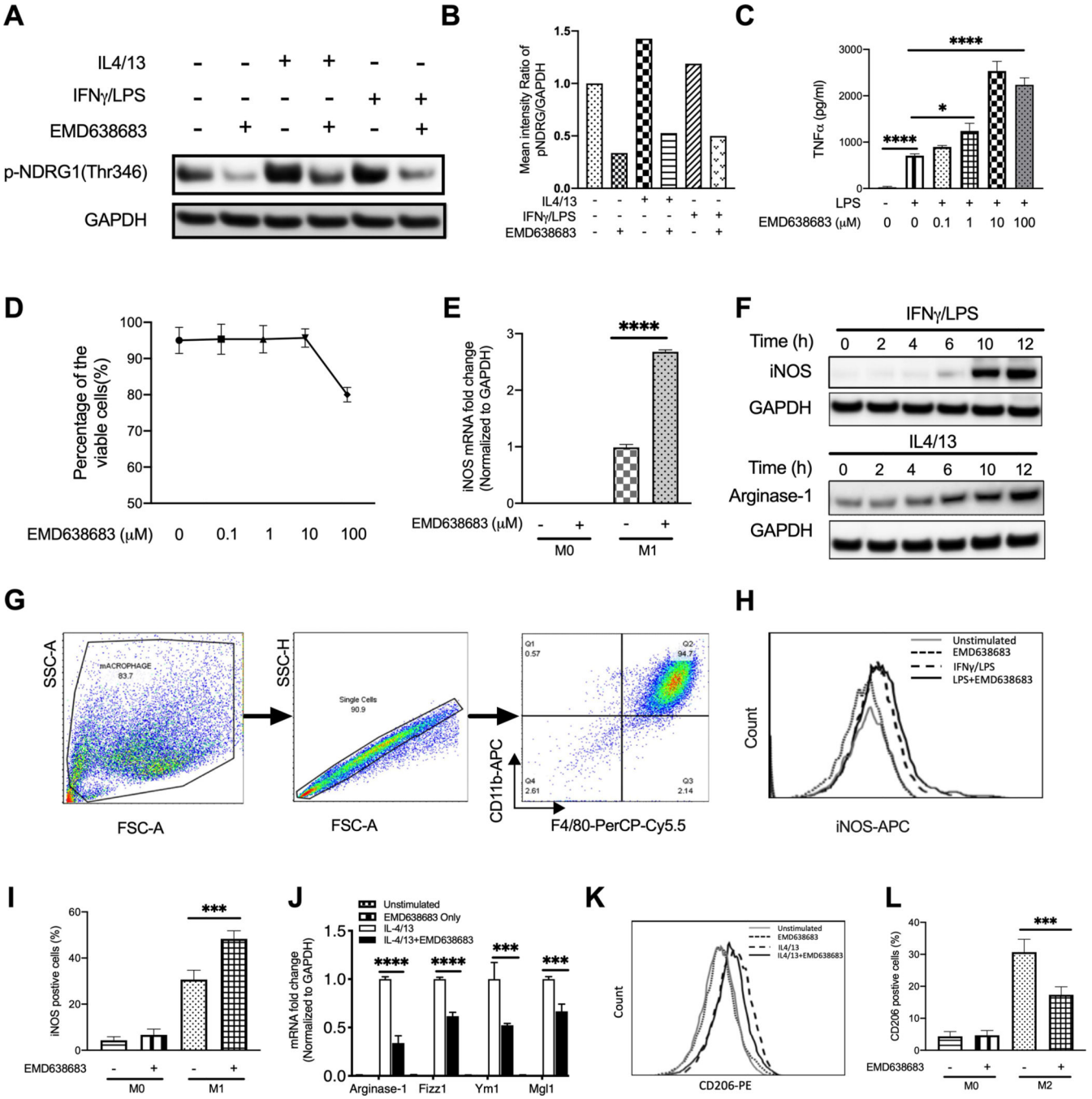

Figure 1. SGK1 differentially regulates transcription of lineage-specific genes in macrophages

BMDMs were stimulated with IFNγ/LPS or IL-4/13 for 24 h in the presence or absence of 10μM EMD638683, then whole cell lysates were collected for analysis. (A) western blots showing the expression of p-NDRG and GAPDH. (B) The ratio of p-NDRG to GAPDH was determined by densitometry quantification assay. BMDMs were pretreated with a serial concentration of EMD638683 followed by the stimulation of *E. coli* LPS and cell-free supernatants were harvested. (C) ELISA showing the production of TNFα in LPS-stimulated BMDMs in the presence or absence of EMD638683. (D) Percentage of

viable cell numbers was calculated after BMDMs were treated with trypan blue for 24 h. (E) qRT-PCR showing the expression of M1-specific macrophage marker, iNOS. (F) western blots showing the dynamic expression of iNOS and arginase-1 in macrophages under M1- or M2- inducing conditions. (G, H and I) BMDMs were stimulated with IFNγ/LPS for 24 h, and monensin was added after 6 h stimulation, then cells were analyzed for intracellular iNOS by flow cytometry. (G) Gating strategy used to obtain pure macrophage populations by selecting CD11b and F4/80 high-expressing cells. (H, I) Flow cytometry showing the influence of EMD638683 on expression of iNOS. (J, K and L) BMDMs were stimulated with IL-4/13 for 24 h in the presence or absence of EMD638683, then qRT-PCR and flow cytometry were used for the next analysis. (J) qRT-PCR showing the effect of EMD638683 on expression of M2-specific macrophage markers Arg1, Ym-1, Mgl-1, and Fizz1. (K, L) Flow cytometry showing the effect of EMD638683 on the expression of CD206. All the blots shown are representative of three to five biological replicates. All data represent the arithmetic mean±S.D. of three independent experiments. *, and *** indicate statistical significance at $P<0.05$ and $P<0.001$, respectively.

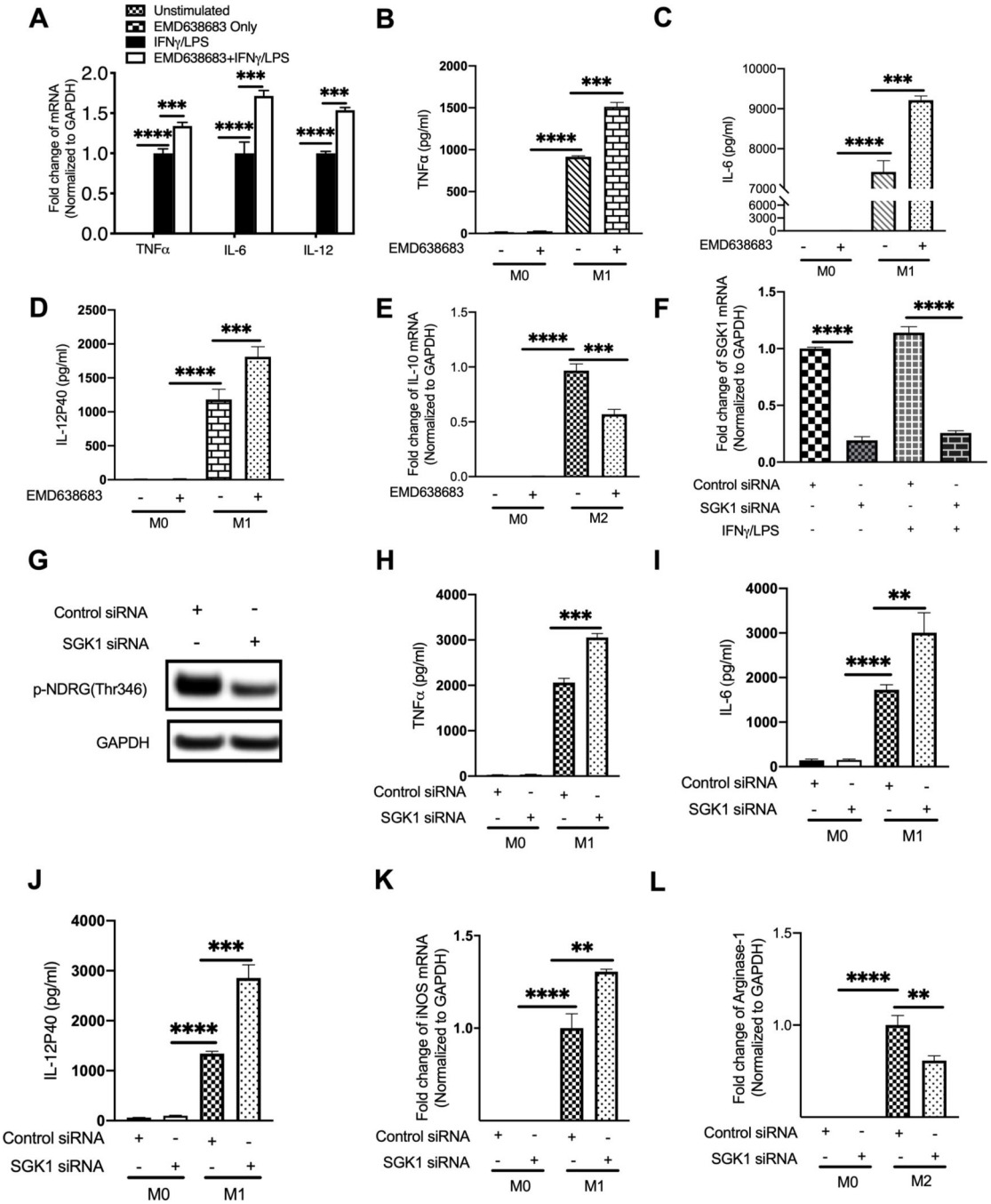

Figure 2. SGK1 suppresses production of M1 macrophage inflammatory cytokines and promotes IL-10 in M2 macrophages

BMDMs were pretreated with 10μM EMD638683 for 2 h or transfected with specific *sgk1* siRNA for 48h and then stimulated with IFNγ/LPS or IL-4/13 for 24 h. (A to D) qRT-PCR and ELISA showing the production of TNFα, IL-6, and IL-12 under the challenge of IFNγ/LPS at message (A) and protein levels (B to D). (E) qRT-PCR showing the effect of EMD638683 on the transcription of IL-10 under the challenge of IL4/13. (F, G) qRT-PCR and western blots showing expression of SGK1 at message (F) and protein (G) levels, respectively, after treatment with *sgk1* siRNA. (H, I and J) ELISA showing the

production of TNFα, IL-6, and IL-12 in *sgk1* gene silencing cells under the challenge of IFNγ/LPS. (K, L) qRT-PCR showing the effect of sgk1 gene silencing on the expression of iNOS and arginase-1 under the challenge of IFNγ/LPS or IL-4/13, respectively. All the data were generated in the same experiment and represent the arithmetic mean±S.D. of three independent experiments. **, ***, and **** indicate statistical significance at $P<0.01$, $P<0.001$, and $P<0.0001$, respectively.

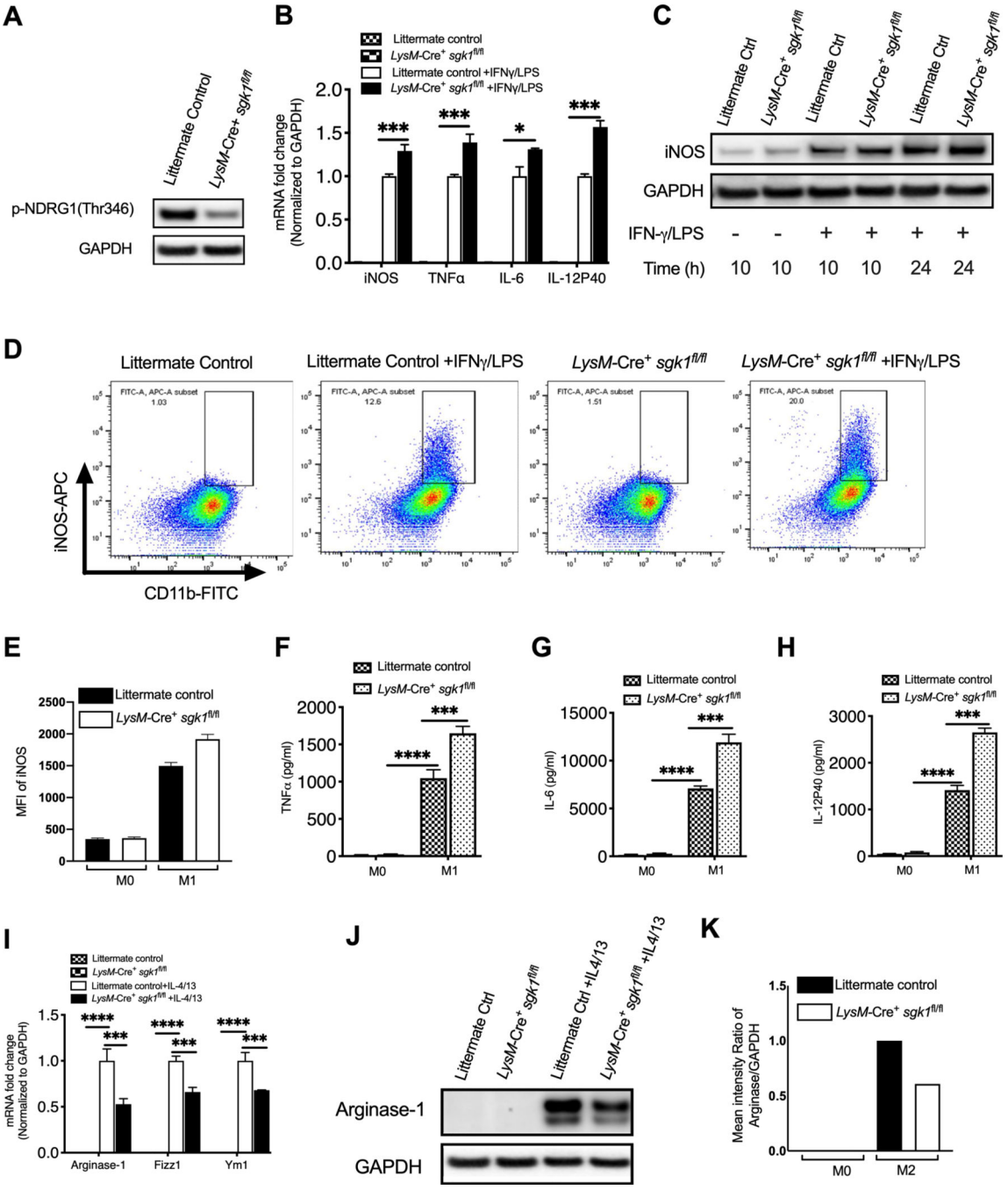

Figure 3. Myeloid lineage-specific deletion of *sgk1* leads to enhancement of M1-like macrophage polarization

LysM-Cre^{+} *sgk1*$^{fl/fl}$ mice were generated by the breeding of *Lys*M-Cre^{+} mice with *sgk1*$^{loxp/loxp}$ mice. Bone marrow from SGK1 knockout and littermate control mice were used to generate BMDMs followed by the treatment with IFNγ/LPS or IL-4/13. (A) Expression of p-NDRG was measured by western blots to assess the knockout efficacy of SGK1 in BMDMs from *LysM*-Cre^{+} *sgk1*$^{fl/fl}$ mice. (B) qRT-PCR showing the message levels of iNOS, and the pro-inflammatory cytokines TNFα, IL-6, and IL-12 under the challenge of LPS/IFNγ. (C, D, and E) western blots and flow cytometry showing expression of iNOS

in the littermate control and *sgk1* knockout BMDMs under the M1 macrophage-inducing conditions. (F, G and H) ELISA showing the production of pro-inflammatory cytokines, TNFα, IL-6, and IL-12 under the M1 macrophage-inducing conditions. (I) qRT-PCR showing the different levels of arginase-1, Ym-1, and Mgl1 in the littermate control and *sgk1*-deficient BMDMs under the M2 macrophage inducing conditions. (J and K) western blots showing the expression of arginase-1 in *sgk1* knockout BMDMs is remarkably higher than in littermate control BMDMs. All the blots shown are representative of three to five biological replicates. All the data represent the arithmetic mean±S.D. of three independent experiments. *, ***, and **** indicate statistical significance at $P<0.05$, $P<0.001$, and $P<0.0001$, respectively

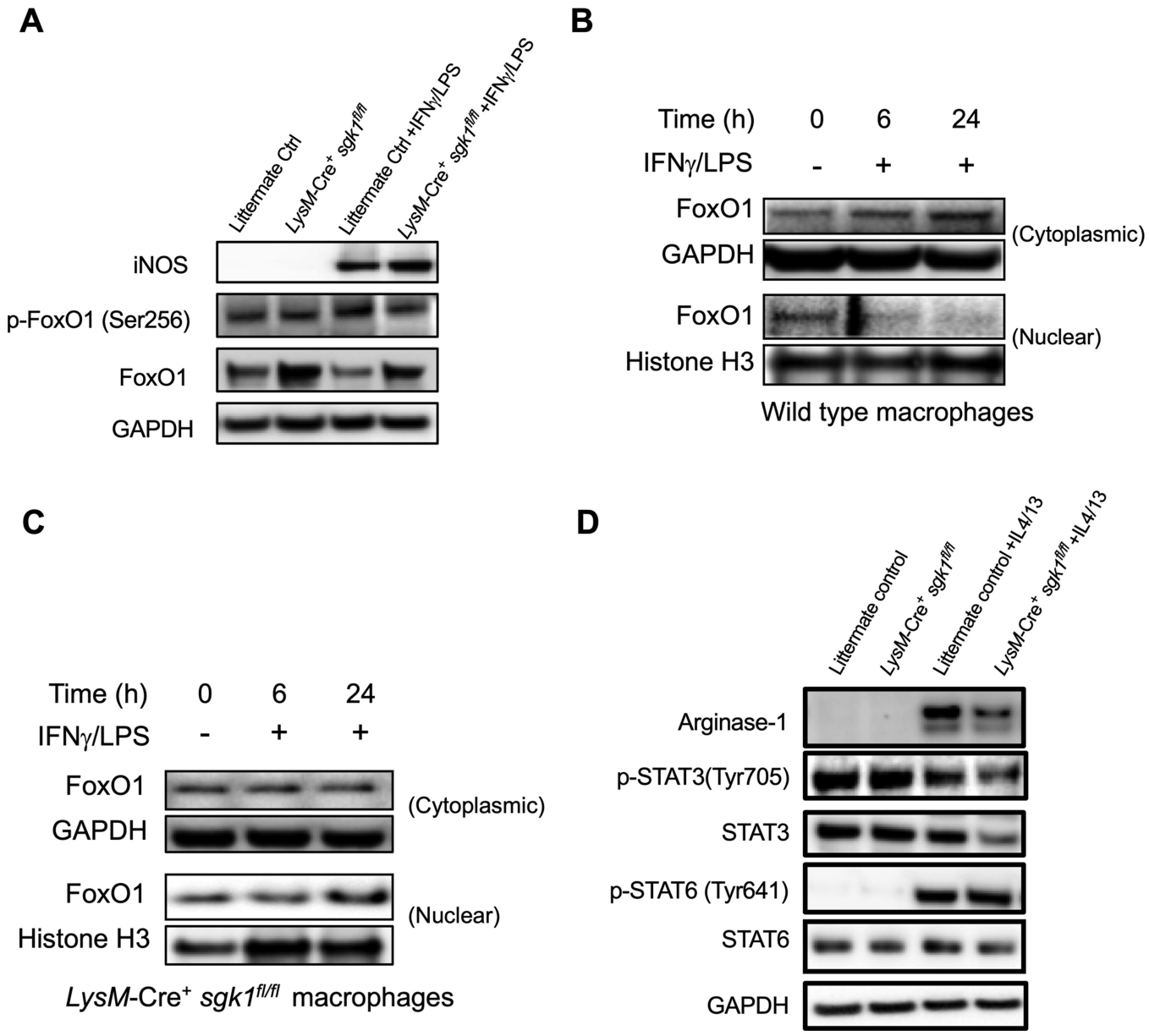

Figure 4. SGK1 differentially regulates expression of FoxO1 and STAT3 in macrophages

BMDMs generated from *LysM*-Cre^{+} *sgk1*$^{fl/fl}$ mice or the littermate control mice were stimulated with IFNγ/LPS or IL-4/13 for the time indicated at day 7, then either the whole cell lysates or the cytoplasmic and nuclear fractions were harvested for western blot assay. (A) western blots showing expression of iNOS, phospho- and total FoxO1, and GAPDH under M1 macrophages inducing conditions. (B, C) Expression of FoxO1 upon the challenge of IFNγ/LPS was measured by western blots, showing the translocation of FoxO1 from the nucleus to the cytoplasm, which restrains LPS-induced inflammatory responses. GAPDH and Histone H3 were used as cytoplasmic and nuclear controls, respectively (B), (C) western blots showing that SGK1 deficiency abrogates the capability of FoxO1 to translocate from the nucleus to the cytoplasm. (D) western blots showing the expression of arginase-1, phospho- and total STAT3, phospho- and total STAT6, and GAPDH under M2 macrophages

inducing conditions. All the blots shown are representative of three to five independent experiments.

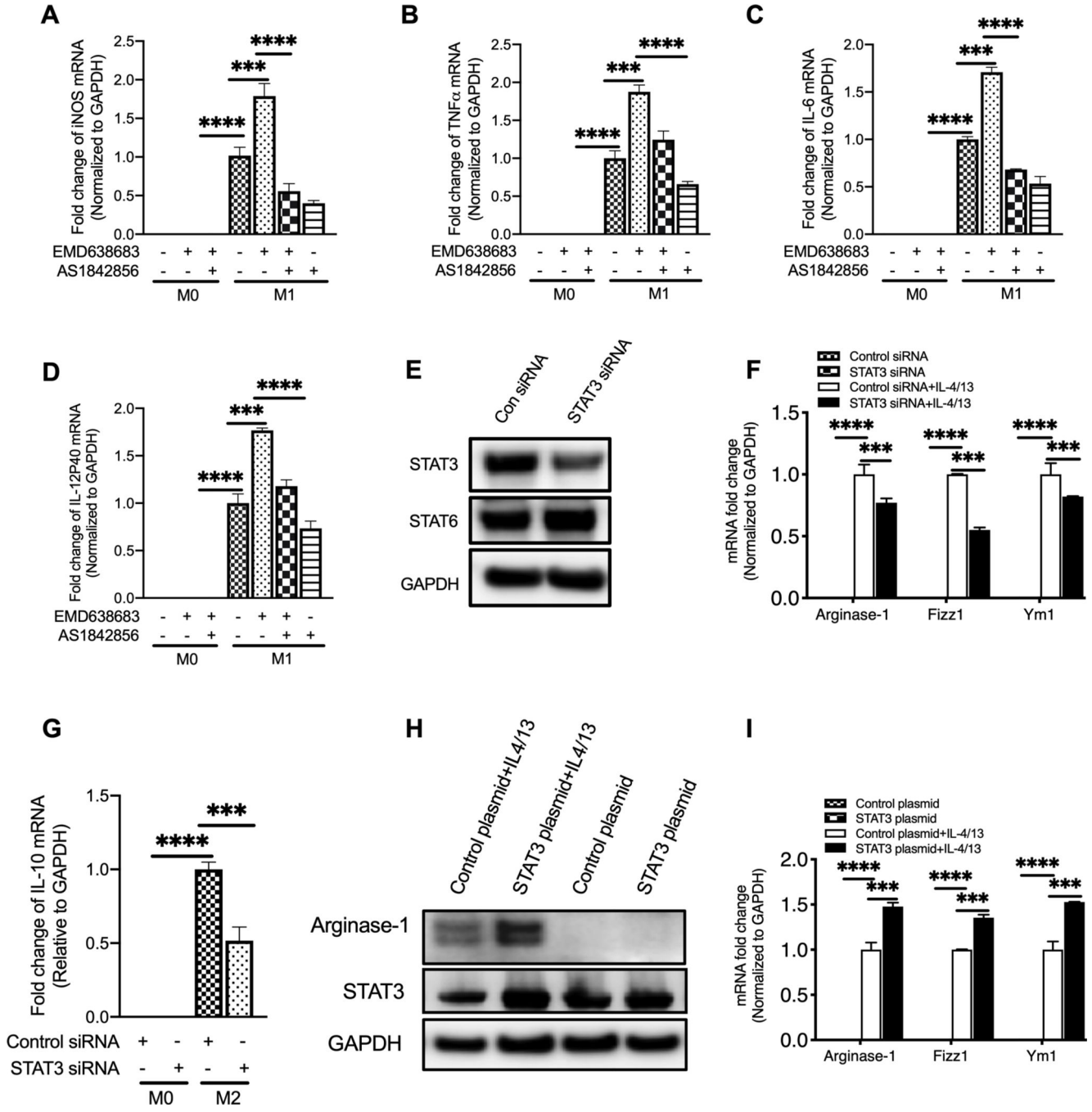

Figure 5. FoxO1 and STAT3 regulate expression of lineage-specific macrophage genes

BMDMs were pre-treated with a FoxO1-specific inhibitor, AS1842856 (10μM), or transfected with specific *stat3* siRNA or a plasmid encoding STAT3 for 48h and then stimulated with IFNγ/LPS or IL-4/13 for 24 h. (A to D) qRT-PCR showing the effect of AS1842856 on iNOS (A), TNFα (B), IL-6 (C), and IL-12 (D) at mRNA levels, indicating FoxO1 inhibition suppresses macrophage polarization towards M1 phenotype. (E, F and G) qRT-PCR showing the silencing of *stat3* (E) significantly decreases arginase-1, Fizz1, Ym1 (F) and IL-10 (G) at mRNA levels under M2 macrophage-inducing conditions. (H,

I) western blots and qRT-PCR showing that overexpression of STAT3 (H) remarkably increases expression of Argniase-1 (H), and significantly increases arginase-1, Fizz1 and Ym1 at message levels (I) under M2 macrophage-inducing conditions. All the data were generated in the same experiment and represent the arithmetic mean±S.D. of three independent experiments. ***, and **** indicate statistical significance at $P<0.001$ and $P<0.0001$, respectively.

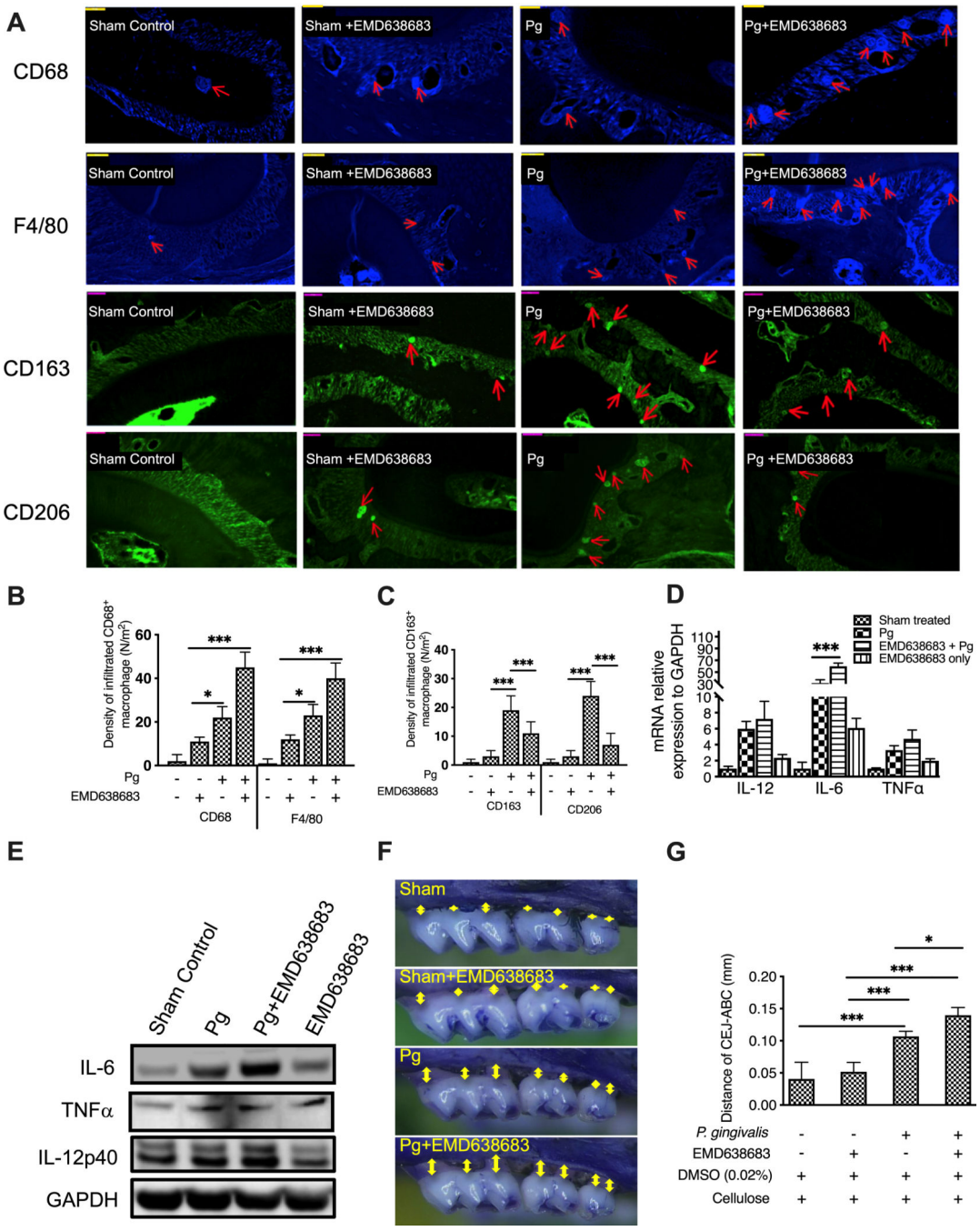

Figure 6. SGK1 promotes M2 macrophage polarization and protects against alveolar bone loss in *P. gingivalis*-infected mice

(A, B) Eight- to 12-week-old C57BL/6 mice were divided randomly into one sham control group and two experimental groups (n=8 per group). The sham control group was treated with cellulose and 0.01% DMSO. The experimental groups were treated with *P. gingivalis* only, *P. gingivalis* with SGK1 inhibitor EMD638683 (15 mg/kg), or treated with inhibitor only. (A) Representative images showing that SGK1 inhibition by EMD638683 robustly elevates expression of CD68 and F4/F80 (Alexa Fluor 350, blue) while concurrently decreasing expression of M2 molecular markers CD206 and CD163 (FITC, green). The

arrows in the images show macrophages being positively stained with CD68, F4/F80, CD163 or CD206. (B to E) Quantification of expression of CD68 and F4/80 (B), and CD206 and CD163 (C), represented with the mean number of positive cells *per* square millimeter that was approximately equal to 5 views under 20X objective. Scale bar = 50μM (D) mRNA levels of TNFα, IL-6, and IL-12P40 were determined by qRT-PCR. (E) Total lysates of gingival tissue from upper jaws were probed for TNFα, IL-6, IL-12P40, and GAPDH. (F) Alveolar bone loss visualized by methylene blue/eosin staining and typical maxillae from sham-infected, *P. gingivalis*-infected, EMD638683 treated, and *P. gingivalis*-infected with EMD638683-treated mice are presented. (G) Quantification of alveolar bone loss represented by the distance from the CEJ to the ABC. Data are presented as the mean CEJ-ABC distance in mm±S.D.; Data are presented as the mean fluorescence density; n=8 mice per group. Error bars represent the S.D. *, and *** indicate statistical significance at $P<0.05$ and $P<0.001$, respectively.

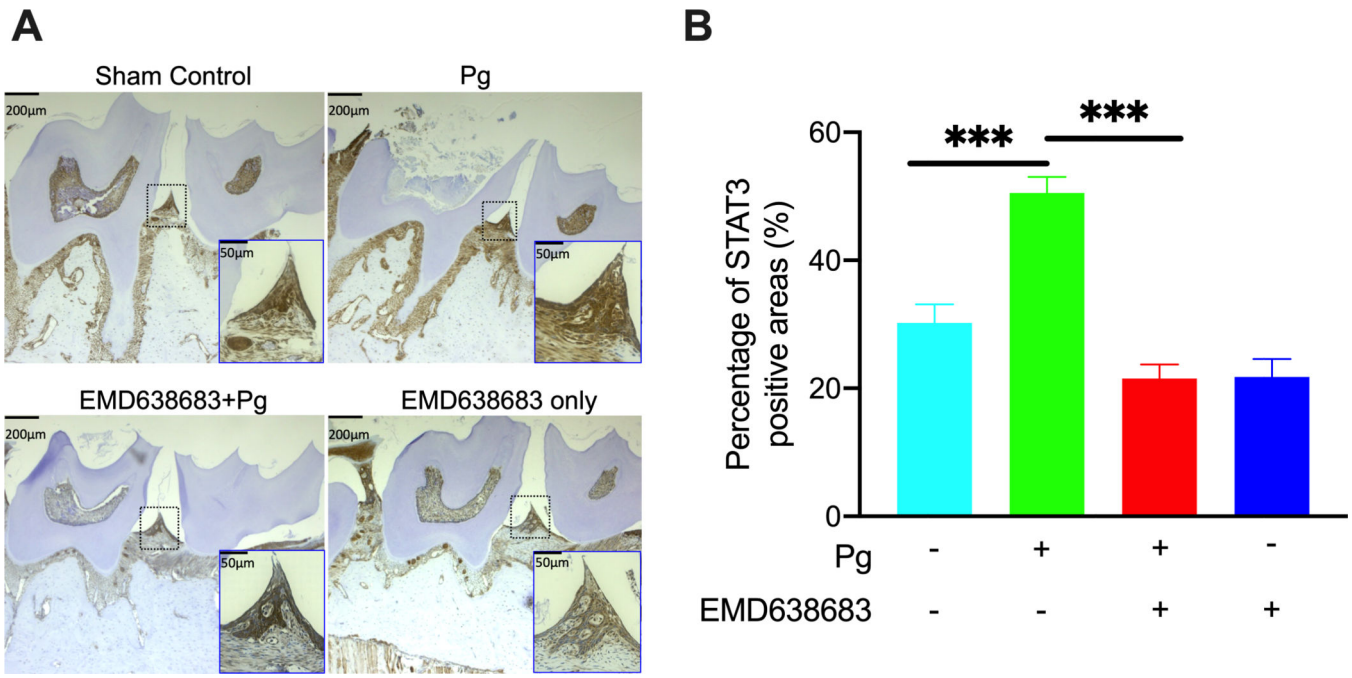

Figure 7. SGK1 regulates expression of STAT3 in *P. gingivalis*-infected mouse gingival tissues

Immunohistochemical staining of serial sections of gingival tissues from experimental mice treated with *P. gingivalis*, *P. gingivalis* plus SGK1 inhibitor (EMD638683, 15mg/kg), or sham control mice treated with DMSO and cellulose with or without EMD638683, showing the expression of STAT3. (A) Representative images showing that *P. gingivalis* infection enhances expression of STAT3 while SGK1 inhibition decreases it in gingival tissue. (B) Quantification of STAT3-positive areas using ImageJ Fiji. Data were derived from analysis of more than 20 microscopic fields of view in at least 5 serial slides. Error bars represent the standard deviation (SD), and "***" indicate statistical significance at $P<0.001$. Data represent the arithmetic mean±SD of three independent experiments.

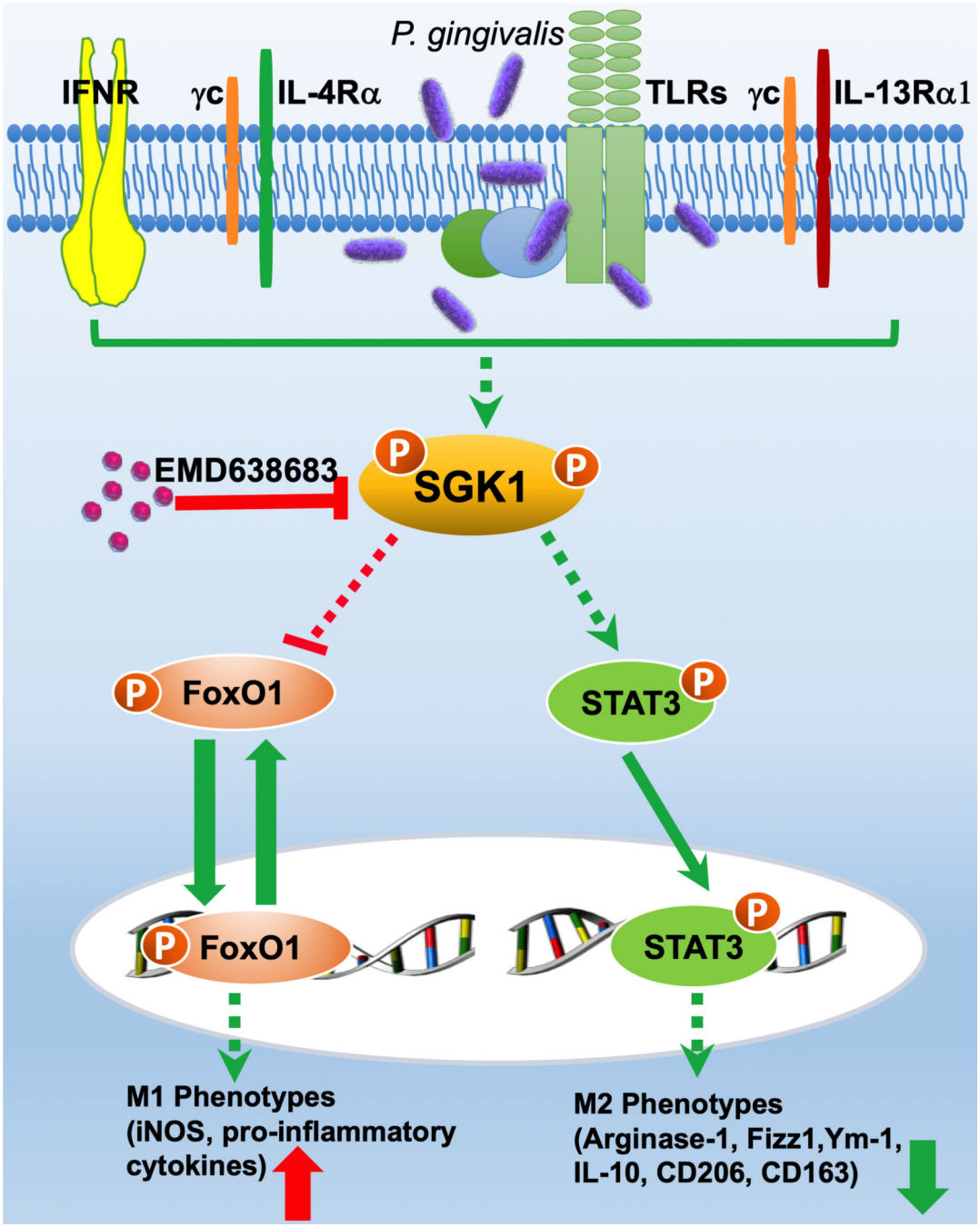

Figure 8. Schematic model of alternative macrophage polarization by SGK1

Activation of SGK1 by external stimuli in the inflammatory milieu restrains FoxO1 activity by facilitating its cytoplasmic translocation, thus decreasing the amount of FoxO1 in the nucleus. Moreover, SGK1 activation increases STAT3 activity, which then promotes macrophage polarization toward M2 phenotypes. In contrast, inhibition of SGK1 decreases STAT3 phosphorylation and reduces its activity. This concurrently abrogates cytoplasmic

translocation of FoxO1, sequestering it in the nucleus, and enhances FoxO1 activity, which drives macrophage polarization toward M1 phenotypes.